

Cleaning of gaseous hydrogen chloride in a syngas by spray-dried potassium-based solid sorbents

Jeom-In Baek^{*,†}, Tae Hyoung Eom^{*}, Joong Beom Lee^{*}, Seong Jegarl^{*}, Chong Kul Ryu^{*},
Young Cheol Park^{**}, and Sung-Ho Jo^{**}

^{*}Future Technology Research Laboratory, KEPCO Research Institute, Daejeon 305-760, Korea

^{**}Greenhouse Gas Research Center, Korea Institute of Energy Research, Daejeon 305-343, Korea

(Received 28 March 2014 • accepted 1 September 2014)

Abstract—There are corrosive gases such as H₂S and HCl in a coal- or biomass-derived syngas. HCl can be removed by Na₂CO₃ or K₂CO₃ at hot temperatures. Hot syngas cleaning has the advantage of improving thermal efficiency. We investigated HCl removal by spray-dried potassium-based solid sorbents which were originally developed for post-combustion CO₂ capture. Both fresh and spent CO₂ sorbents were tested to confirm the applicability as a sorbent for HCl cleaning. Saturation chlorine sorption capacity was measured using a fixed-bed reactor at a temperatures of 300-500 °C under an ambient pressure. Both fresh and spent CO₂ sorbents showed saturation chlorine sorption capacity above 15 wt%. HCl removal performance of the sorbents was investigated in a micro fluidized-bed reactor and a bench-scale bubbling fluidized-bed reactor. HCl concentration was lowered from 150-900 ppmv to less than 5 ppmv and from 130-390 ppmv to less than 1 ppmv in a micro fluidized-bed reactor and in a bench-scale bubbling fluidized-bed reactor, respectively, at 300-540 °C and 20 bar. It could be concluded that both fresh and spent spray-dried potassium-based CO₂ sorbents could be utilized as a disposable HCl sorbent for hot syngas cleaning.

Keywords: Syngas, Hot Gas Cleaning, Hydrogen Chloride, Sorbent, Fluidized-bed Reactor

INTRODUCTION

Integrated gasification combined cycle (IGCC) power plants with pre-combustion CO₂ capture are evaluated to have higher thermal efficiency than pulverized coal-fired (PC) power plants with post-combustion CO₂ capture [1,2]. Although an IGCC power plant with CO₂ capture based on currently available commercial technologies is an attractive power generation system, the thermal efficiency loss of around 7.5% caused by the CO₂ capture is still too high to be accepted in the market [1,2]. Several new technologies, such as advanced gas turbine, ion transport membrane, hydrogen membrane, hot syngas cleaning, and coal feed pump, are under development to improve the efficiency of the IGCC power plant [3]. It is estimated that hot syngas cleaning can improve the thermal efficiency of IGCC by more than 2% [4].

Coal- or biomass-derived syngas contains contaminant gases such as H₂S, HCl, NH₃, Hg, As, Se, etc. These gases should be purified to protect the equipment through which the syngas passes or to meet environmental regulations. For hot syngas cleaning, solid sorbents working at a temperature range of 200-500 °C should be developed. A large portion of the sorbent studies for the hot syngas cleaning was focused on desulfurization sorbents because of high concentration (1,000-10,000 ppmv) of sulfur compound among the contaminant gases. Usually zinc-based sorbents are used for sulfur purification from syngas [5-8]. Hydrogen chloride (HCl) is

another major contaminant gas and its concentration in the syngas is 40-700 ppmv [9]. Purification of HCl to the level of parts-per-million (ppm) is required for the applications to IGCC and to the level of parts-per-billion (ppb) for fuel-cell or chemicals production applications.

Alkali- and alkaline earth metal-based solid sorbents, especially sodium-based or calcium-based sorbents, have been intensively investigated due to their excellent HCl capture efficiency. Studies on the CaO or CaCO₃ sorbents were usually conducted for the applications above 500 °C [10-13]. Duo et al. [14] reported that CaCO₃ is a poor HCl sorbent in syngas around 400 °C, and they found that HCl sorption of Na₂CO₃ is more effective at 400-500 °C than at either 300 or 600 °C. Verdone et al. [15] also suggested that HCl capture efficiency of a Na₂CO₃ sorbent reaches maximum values at 400-500 °C. Dou et al. [16,17] removed HCl from 640 ppm to below 1 ppm at 550 °C with the sorbent containing mixed Na-, Ca- and Mg-based compounds in a fixed-bed reactor. The sorbent showed higher chlorine sorption capacity at higher temperatures between 300 and 650 °C. Ohtsuka et al. [9] tested NaAlO₂ as an HCl sorbent in a fixed-bed reactor. It removed HCl in a simulated syngas from 200 ppm to below 1 ppm at 400 °C. The HCl removal efficiency of NaAlO₂ was better than that of Na₂CO₃. Both NaAlO₂ and Na₂CO₃ showed reduced chlorine sorption capacity under the presence of H₂S. As an effort to find inexpensive sorbent, Krishnan et al. [18] tested nahcolite (NaHCO₃), which is a natural carbonate mineral and transformed to porous Na₂CO₃ at temperatures above 150 °C. The nahcolite-based sorbent reduced HCl concentration from 1,750 ppm to below 1 ppm at 400-600 °C in a fixed-bed reactor. Although Na₂CO₃ and K₂CO₃ have been reported to

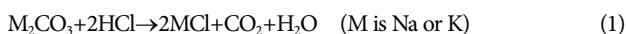
[†]To whom correspondence should be addressed.

E-mail: perbaek@kepco.co.kr

Copyright by The Korean Institute of Chemical Engineers.

have equilibrium HCl pressures of <1 ppm at $\leq 500^\circ\text{C}$ [18,19], the studies on the HCl removal by K_2CO_3 -based sorbents at hot temperatures and high pressures for fluidized-bed applications are hardly found.

Korea Electric Power Corporation Research Institute (KEPCO RI) has been developing spray-dried solid sorbents for hot syngas cleaning and CO_2 capture in a fluidized-bed process [20-23]. KEPCO RI's dry regenerable CO_2 sorbents for post-combustion CO_2 capture uses Na_2CO_3 or K_2CO_3 as an active component. These sorbents can be used as HCl sorbents because Na_2CO_3 and K_2CO_3 are also the active components of an HCl sorbent. The reaction between Na_2CO_3 or K_2CO_3 and HCl is as follows:



In this study, we measured saturation chlorine sorption capacities of spray-dried potassium-based CO_2 sorbents in a fixed-bed reactor under ambient pressure. In addition, HCl removal tests were conducted in a micro fluidized-bed reactor, and in a bubbling fluidized-bed reactor under high pressure using simulated syngas. The HCl removal performance of a spent CO_2 sorbent was also tested to confirm its reusability as an HCl sorbent for hot syngas cleaning.

EXPERIMENTAL

1. Preparation of Sorbents

All sorbents tested were prepared by a spray drying technique that is easily scalable to commercial quantity and can produce a large amount of sorbent with uniform property suitable for fluidized-bed applications. In this study, the solid raw materials for the preparation of the sorbents consist of active materials, support, and inorganic binders. The active material was K_2CO_3 and its initial content in the raw materials was 35 wt%. $\gamma\text{-Al}_2\text{O}_3$ was the major component of the raw support material. The solid raw materials were well mixed in pure water added with organic additives such as dispersant, defoamer, and organic binder. The mixed slurry was comminuted with ball mill to make a homogeneous colloidal slurry. The homogenized slurry was spray-dried to form spherical particles, i.e., green body. The green body was calcined at $550\text{--}750^\circ\text{C}$ in a muffle oven for 3 h under air atmosphere after pre-drying at 120°C overnight. The organic additives were burned out during the calcination. The prepared sorbent was named as HK-1. Sorbent HK-1S is a spent sorbent of HK-1. HK-1S was taken from the 0.5 MW CO_2 capture pilot plant, which is installed in a coal-fired power plant, after operation with HK-1 for one month to capture CO_2 from flue gas. Sodium-based sorbent, Sorbent HN-1, was additionally prepared for comparison purposes following the same procedure of the HK-1 preparation. The initial content of Na_2CO_3 in the raw materials was 30 wt%.

2. Characterization of Sorbents

The shape of calcined sorbents was examined by scanning electron microscope (SEM) images. Average particle size of the sample was measured using standard sieves and a sieve shaker (Meinzer II, CSC Scientific Company). The measuring procedure for particle size and size distribution was followed by the American Society for Testing and Materials (ASTM) E-11 method. 10 g of sorbent

was sifted for 30 minutes using sieve shaker mounted with the stacked standard sieves. The weight of sorbent on each sieve was measured and the average particle size and size distribution were calculated with the obtained data. Packing density or tapped density of each sorbent was measured using the Autotap instrument (Quantachrome) proposed in ASTM D 4164-88. 250 ml of sorbent was tapped for 1000 times and then the packing density was determined by dividing the sorbent mass by its tapped volume. Brunauer-Emmett-Teller (BET) surface area of the sample was determined by N_2 physisorption using an ASAP 2420 (Micromeritics Inc.) automated system. Attrition resistance or mechanical strength of the calcined sorbents was measured with a modified three-hole air-jet attrition tester based on the ASTM D 5757-95. Attrition resistance was determined at 10 standard L/min (slpm) over 5 h as described in the ASTM method. Attrition index (AI) or attrition loss is the percent fines generated over 5 h. The fines are particles less than $40\ \mu\text{m}$ collected at the thimble, which is attached to the gas outlet, after 5 h from the start.

$$\text{AI} = [\text{total fine collected for 5 h} / \text{amount of initial sample (50 g)}] \times 100\% \quad (2)$$

A lower AI indicates higher attrition resistance of the particles. The AI of fresh Akzo fluid catalytic cracking (FCC) catalyst, which was used as a reference, was 22.5%, under the same measurement condition.

3. Reactivity Measurement

Saturation chlorine sorption capacity of the sorbents was measured using a fixed-bed reactor under ambient pressure. We used automated catalyst characterization system (Micromeritics, AutoChem II 2920), which consists of gas feeding section, a fixed-bed reactor placed in an electrically heated furnace, and gas analysis section. Around 0.8 g of sorbent was packed in the fixed-bed reactor made of quartz tube. The inner diameter of the reactor was 9.9 mm. A simulated syngas containing HCl (20 vol% H_2 , 3 vol% N_2 , 2,500 ppmv HCl, and CO balance) was continuously introduced by mass flow controllers until the HCl concentration in outlet gas reached the inlet HCl concentration. The flow rate of the simulated syngas was 100 ml/min. The variation of gas concentration by the reaction was monitored with mass spectrometer (Pfeiffer Vacuum, OmniStar). Saturation chlorine capacity of the sorbents was calculated by obtaining Cl^- ion concentration after dissolution of the Cl-saturated sorbents in water. Quantitative analysis of Cl^- was performed using an ion chromatograph (IC, Dionex DX-120), which was equipped with a Dionex IonPac AS 14 (4 mm \times 250 mm) column and a conductivity detector. The eluent solution was 3.5 mM Na_2CO_3 /1 mM NaHCO_3 . Phase identification of the sorbents before and after reaction was done by multi-purpose X-ray diffractometer (Rigaku, Japan).

HCl removal performance of the sorbents at high pressure was measured with a micro fluidized-bed reactor and a bench-scale bubbling-fluidized-bed reactor. The system configuration of both reactor systems is similar to that of the fixed-bed reactor system except for gas analysis section. The detailed experimental conditions used in fluidized-bed reactor tests are summarized in Table 1. At high pressure tests, HCl concentration was monitored with Fourier transform infrared spectroscopy (FT-IR) gas analyzer (GAS-MET, DX-4000) of which operating temperature is 180°C . All the

Table 1. Experimental conditions for fluidized-bed reactor

	Micro reactor	Bench-scale reactor	
		Experiment I	Experiment II
Temperature / °C	300, 400, 500	400, 460-540	300, 460
Pressure / bar	20	5, 20	20
Sorbent inventory / g	2, 3, 4	400	100
Gas velocity / (m/s)	-	0.03	0.02
Gas flow rate (STP) / (L/min)	1.0	-	-
Gas composition / vol%	H ₂ 30%, CO ₂ 6%, CO balance	N ₂	N ₂
Inlet HCl concentration / ppmv	150, 370, 900, 1800	130, 230, 280	390

gas lines downstream the reactor were heated to 180 °C to prevent water vapor condensation and HCl dissolution into the condensed water and to minimize the HCl deposition on the surface of gas lines. A simulated syngas was used in the micro fluidized-bed reactor tests and nitrogen containing HCl in the bench-scale bubbling-fluidized-bed reactor tests. In the tests of bench-scale bubbling-fluidized-bed reactor, the flow rate of simulated syngas was adjusted to maintain constant gas velocity when the reaction temperature was changed. The inner diameters of micro reactor and bench-scale reactor are 0.8 and 50 mm, respectively. For the micro reactor tests, breakthrough was determined when the outlet HCl concentration reached 10 ppmv and the breakthrough chlorine sorption capacity was calculated from the gas concentration data obtained by the FT-IR analyzer. The effects of HCl concentration, reaction temperature, and pressure were investigated.

RESULTS AND DISCUSSION

1. Physical Properties of Sorbents

The physical properties of the spray-dried sorbents are summarized in Table 2. HN-1 and HK-1 had excellent physical properties suitable for fluidized-bed applications. The shape of HN and HK sorbents was spherical as shown in Fig. 1. The sorbents had average particle size of 100-125 μm. The size distribution and bulk density of the sorbents were 42-355 μm and 0.8-1.0 g/mL, respectively, which are suitable values for fluidized-bed applications.

The attrition resistance is the most important criterion among physical properties which decides the applicability of the sorbent for a fluidized-bed process. Sorbents with AI above 60% are not suitable for bubbling fluidized-bed reactor and those with AI above 30% are not suitable for transport reactor. Sorbents HN-1 and HK-1

Table 2. Physical properties of the sorbents

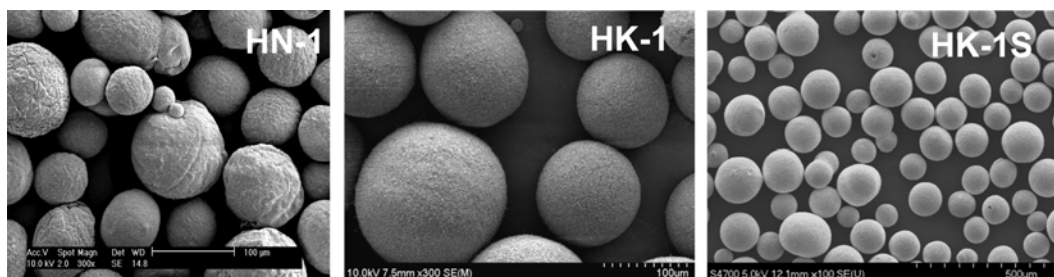
	HK-1	HK-1S	HN-1
Shape	Sphere	Sphere	Sphere
Average particle size / μm	104	108	121
Particle size distribution / μm	42-355	42-355	42-355
Bulk density / (g/ml)	0.98	0.96	0.84
BET surface area / (m ² /g)	39.3	13.6	64.3
Attrition index / %	<0.1	0.6	4.7

turned out to have high attrition resistance. Their AI values less than 5% are much lower than that of commercial FCC catalyst (22.5%). The spent sorbent, HK-1S, still maintained its physical properties including high mechanical strength after one month operation for CO₂ capture.

2. Saturation Chlorine Sorption Capacity of Sorbents

A good HCl sorbent should remove HCl almost completely to the level of a few ppmv for combined cycle power generation, and it should have a large HCl sorption capacity for long term use. Saturation of HCl on the sorbents was carried out in the fixed-bed reactor under ambient pressure and 300-500 °C. The concentration of HCl at the outlet of the fixed-bed reactor was drastically reduced to near zero level as soon as the reactant gas flowed into the reactor packed with sorbent, which clearly indicates that HCl absorption takes place rapidly and completely by the sorbent. HCl sorption continued longer than 10 h for most sorbents with maintaining the outlet concentration of HCl to near zero level.

The saturation chlorine sorption capacity of the sorbents taken from the fixed-bed reactor was determined on the basis of Cl⁻ ion concentration after dissolution of HCl-saturated sorbents in water.

**Fig. 1. SEM images of the sorbents.**

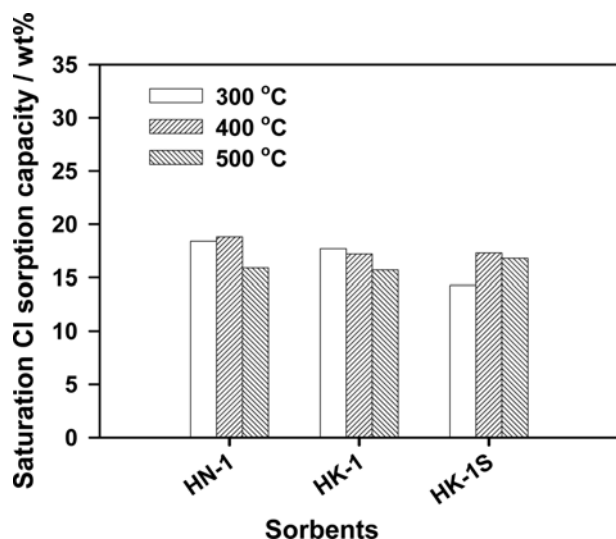


Fig. 2. Saturation chlorine sorption capacities of tested sorbents at different reaction temperatures.

Fig. 2 compares saturation chlorine sorption capacities of the sorbents at different experimental temperatures. The saturation chlorine sorption capacity of the sorbents was in the range of 15 to 19 wt%. It was observed that the saturation sorption capacity was reduced moderately as the reaction temperature increased. The utilization

rates of active component of the sorbents at 500 °C were 79.1 and 87.2% for HN-1 and HK-1, respectively. Potassium-based sorbents showed higher utilization rate of active component. There was not much difference in the saturation chlorine sorption capacity between sorbent HK-1 and spent sorbent HK-1S as shown Fig. 2.

To verify the reaction in Eq. (1) under experimental conditions, X-ray diffraction analysis of the sorbents was performed. Fig. 3 shows XRD patterns of Na-based and K-based sorbents before and after HCl absorption at different temperatures. In the fresh sorbent HN-1 and HK-1, sodium and potassium existed in the form of Na_2CO_3 or $\text{Na}_2\text{CO}_3 \cdot \text{H}_2\text{O}$ and K_2CO_3 or $\text{K}_2\text{CO}_3 \cdot 1.5\text{H}_2\text{O}$, respectively. It is assumed that the hydrates of Na_2CO_3 and K_2CO_3 were formed by absorbing water vapor in the air. The hydrates lost the water while they are heated to the experimental temperatures for HCl absorption. After HCl absorption, almost all peaks of Na_2CO_3 or $\text{Na}_2\text{CO}_3 \cdot \text{H}_2\text{O}$ in HN-1 and K_2CO_3 or $\text{K}_2\text{CO}_3 \cdot 1.5\text{H}_2\text{O}$ in HK-1 disappeared and NaCl and KCl peaks were observed. This clearly shows that absorbed chlorine on HN-1 and HK-1 formed NaCl and KCl, respectively. The XRD patterns of spent sorbent, HK-1S, are shown in Fig. 4. The major peaks of HK-1S before HCl absorption were K_2CO_3 and $\text{K}_2\text{CO}_3 \cdot 1.5\text{H}_2\text{O}$, and low KAlSiO_4 peaks were observed. It is estimated that KAlSiO_4 was formed by the combination of potassium with aluminum and silica originated from K_2CO_3 , support and binder, respectively, during the cyclic CO_2 absorption and regeneration. KAlSiO_4 peaks still remained after HCl absorption, indicating KAlSiO_4 does not react with HCl. $\text{K}_2\text{CO}_3 \cdot 1.5\text{H}_2\text{O}$ is easily de-

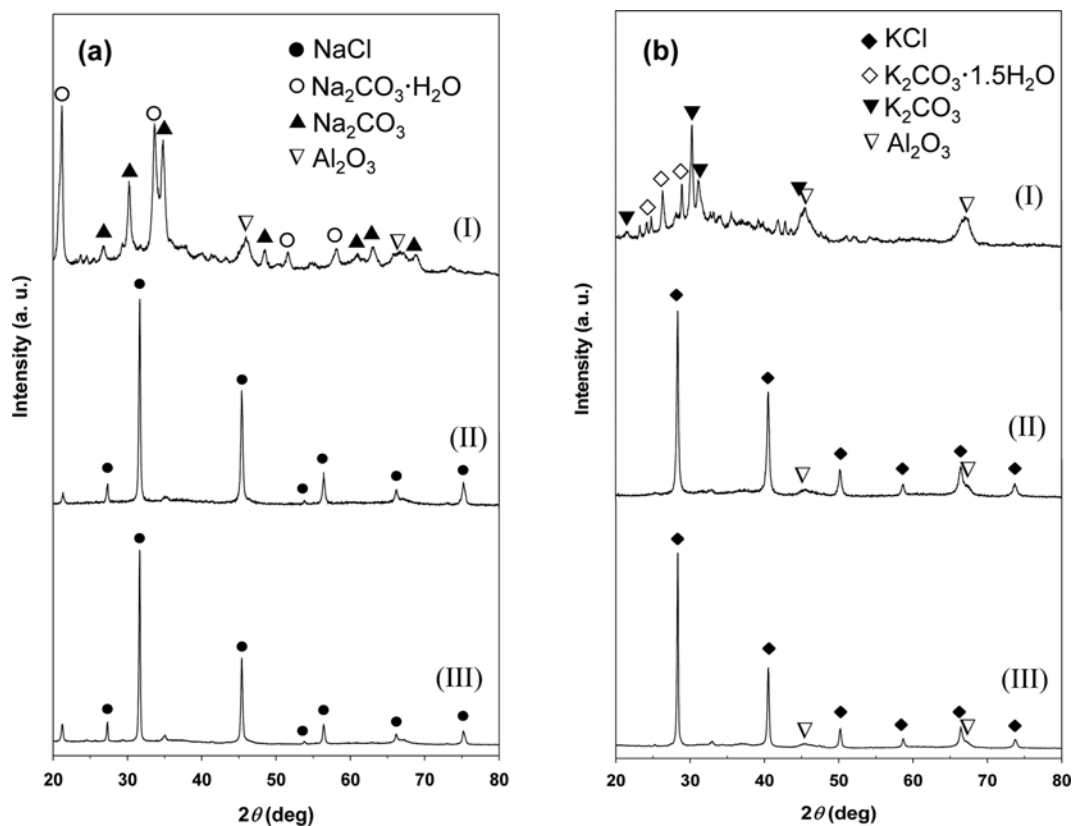


Fig. 3. XRD patterns of sorbents (a) HN-1 and (b) HK-1 before and after HCl absorption reaction: (I) before reaction, (II) after reaction at 300 °C, and (III) after reaction at 500 °C.

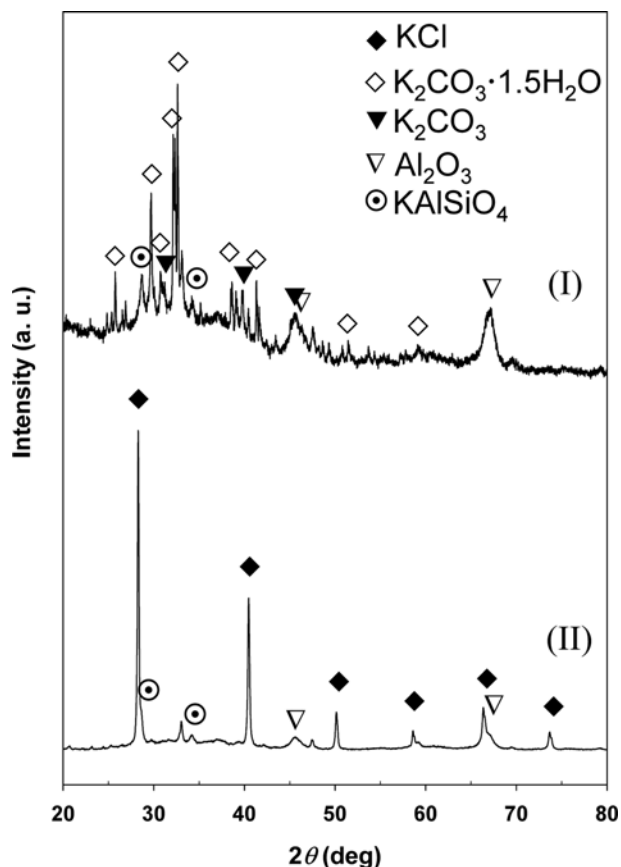


Fig. 4. XRD patterns of sorbents HK-1S before and after HCl absorption reaction: (I) before reaction and (II) after reaction.

composed into K_2CO_3 and water vapor when it is heated above $100^\circ C$ even though the decomposition temperature increases when surrounding water vapor concentration is high. $KHCO_3$, which is formed by the CO_2 absorption reaction ($K_2CO_3 + CO_2 + H_2O \leftrightarrow 2KHCO_3$), was not observed. This indicates that the sorbent was sufficiently regenerated in the regeneration reactor of the pilot CO_2 capture facility. Even if $KHCO_3$ exists in the sorbent by insufficient regeneration, it is decomposed into K_2CO_3 , CO_2 , and H_2O under $250^\circ C$ while the sorbent is heated up to the reaction temperature above $300^\circ C$ for HCl cleanup. K_2CO_3 derived from the decomposition of $KHCO_3$ and $K_2CO_3 \cdot 1.5H_2O$ reacts with HCl to form KCl. Therefore, the peaks of $K_2CO_3 \cdot 1.5H_2O$ and $KHCO_3$ disappear and KCl peaks are observed in the XRD patterns after HCl absorption as shown in Fig. 3(b) and 4. The XRD analysis result of spent sorbent, HK-1S, confirms that spent spray-dried K_2CO_3 -based CO_2 sorbents can absorb HCl successfully to form KCl.

3. HCl Removal Performance of Sorbents in the Fluidized-bed Reactors

Fig. 5 shows the breakthrough curves of HK-1, HK-1S, and HN-1 sorbents in the micro fluidized-bed reactor tests at 20 bar and 300– $500^\circ C$. The outlet concentration of HCl was sharply reduced as soon as the reactant gas passed through the sorbent, which was placed on the porous filter. Although HN-1 removed HCl to a few ppmv level, HK-1 and HK-1S sorbents were not able to remove HCl concentration of around 900 ppmv below 10 ppmv at $500^\circ C$

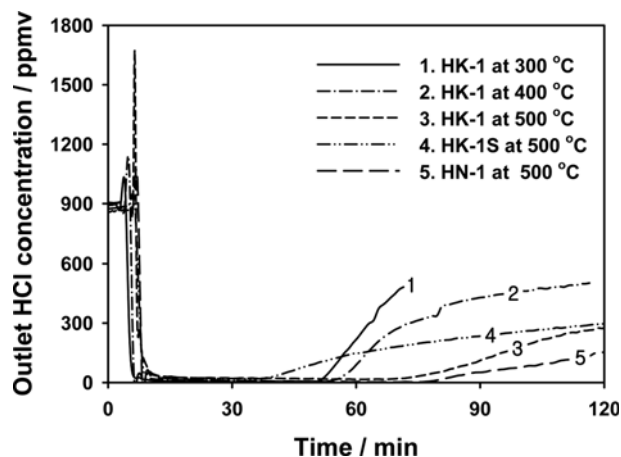


Fig. 5. The breakthrough curves of the sorbents in the micro fluidized-bed reactor at 20 bar; 2 g sorbent; gas composition: H_2 30%, CO_2 6%, CO balance.

due to the insufficient contact time. The lowest concentrations during HCl absorption by HK-1 and HK-1S were 16.1 and 18.4 ppmv, respectively, at $500^\circ C$. When reaction temperature was lowered to 300 or $400^\circ C$, the outlet HCl concentrations by HK-1 sorbent were 5.4 and 2.9 ppmv, respectively, due to the increased contact time and a lower equilibrium concentration of HCl in the gas with K_2CO_3 on the sorbent at lower temperatures. At a lower reaction temperature, faster breakthrough of HCl sorption was observed. HCl removal performance of sodium-based sorbent, HN-1, was superior to that of potassium-based sorbents. It reduced outlet HCl concentration to 2.3 ppmv even at $500^\circ C$ and maintained the low HCl concentration for a longer time compared with the potassium-based sorbent, HK-1. It is estimated that higher surface area and a little higher breakthrough chlorine sorption capacity of HN-1 contributed to the better HCl cleaning performance of HN-1.

To investigate the possibility of HCl removal to a few ppmv level by the spent potassium-based CO_2 sorbent, HK-1S, at $500^\circ C$ and inlet HCl concentration of around 900 ppmv, we conducted HCl removal tests with changing sample amount. As the amount of HK-1S increased from 2 g to 3 g and 4 g, the outlet HCl concentration reduced to 4.7 and 2.4 ppmv, respectively. This indicates that sorbent HK-1S can reduce HCl to a few ppmv levels even at $500^\circ C$ as long as sufficient contact time is provided.

The breakthrough chlorine sorption capacity of the sorbents at 20 bar was calculated from the outlet HCl concentration data obtained by the gas analyzer. The volume of HCl absorbed in the sorbents was integrated until the outlet HCl concentration reached to breakthrough concentration of 10 ppmv. If the HCl concentration was not lowered below 10 ppmv, the breakthrough was defined as the point at which the outlet HCl concentration started to increase after maintaining a low level HCl emission period. The breakthrough chlorine sorption capacities at 20 bar and $500^\circ C$ were summarized in Table 3 with the saturation sorption capacities obtained in the fixed-bed tests at ambient pressure. Sodium-based sorbent, HN-1, showed a little higher breakthrough chlorine sorption capacity compared with potassium-based sorbents at the same experimental condition, utilizing 24.8% of active component at breakthrough

Table 3. Chlorine sorption capacity of sorbents

	Experimental condition				Chlorine sorption capacity mmol/g sorbent		
	Temperature	Pressure	Sorbent amount	Inlet HCl	HN-1	HK-1	HK-1S
	/ °C	/ bar	/ g	concentration / ppmv			
Saturation sorption capacity	500	0	2	900	4.49	4.43	4.74
Breakthrough sorption capacity	500	20	2	900	1.41	1.21	0.59
	500	20	3	900			1.18
	500	20	4	900			1.24
	500	20	2	150			0.28
	500	20	2	370			0.42
	500	20	2	1800			0.70

point. The spent sorbents, HK-1S, showed lower breakthrough chlorine sorption capacity than the fresh one. However, the breakthrough chlorine sorption capacity of HK-1S increased to a value similar to that of fresh one when the sorbent amount used increased, which indicates that the breakthrough chlorine sorption capacity of HK-1S can be improved if sufficient contact time between the reactant gas and sorbent are obtained. The utilization rates of active component of HK-1S at breakthrough point were 11.7 and 24.5% for the tests at 2 and 4 g sorbent use, respectively.

The effect of inlet HCl concentration on the breakthrough curve of HK-1S was investigated in the micro fluidized-bed reactor at 20 bar and 500 °C. At a low inlet HCl concentration (150 and 370 ppmv), a low outlet HCl concentration of around 6 ppmv was achieved, even at 500 °C by 2 g sorbent. However, the breakthrough chlorine sorption capacity decreased with decreasing the inlet HCl concentration as shown in Table 3, which implies that the reaction is limited by the mass transfer. From the results on the effects of sorbent amount used and inlet HCl concentration, it is estimated that the outlet HCl concentration of a few ppmv level at 20 bar and 500 °C can be achievable by HK-1S at the HCl space velocity below $3 \text{ mL HCl} \times \text{g}_{\text{sorbent}}^{-1} \times \text{h}^{-1}$.

The HCl removal test in a bench-scale bubbling fluidized-bed reactor was conducted with HK-1S to verify the HCl removal performance of a spent CO₂ sorbent. The amount of sorbent in the reactor was 400 g and gas velocity of 0.03 m/s was maintained. In

this condition, contact time between reactant gas and sorbent was around 7 s. HK-1S removed HCl below 1 ppmv at 400 °C and both 5 and 20 bar for inlet HCl concentration of 130 and 230 ppmv. During the temperature increase from 460 to 540 °C, the outlet HCl concentration was still maintained below 1 ppmv at 20 bar for inlet HCl concentration of 280 ppmv as shown in Fig. 6. At a reduced sorbent amount of 100 g and gas velocity of 0.2 m/s, at which the contact time between reactant gas and sorbent was around 3 s, the outlet concentration of HCl was still maintained below 1 ppmv at 20 bar and both 300 and 460 °C for inlet HCl concentration of 390 ppmv. The HCl removal test results in the bench-scale bubbling fluidized-bed reactor also suggest that the spent CO₂ sorbents can be used as an HCl sorbent to remove HCl to a few ppmv level.

CONCLUSIONS

The HCl removal performance of a spray-dried sorbents, which were originally developed for post combustion CO₂ capture, was investigated in the hot temperature zone. Sodium- and potassium-based sorbents, HN-1 and HK-1, respectively, showed excellent physical properties suitable for fluidized-bed process applications. Both sorbents showed high saturation chlorine sorption capacity above 15 wt%, utilizing more than 80% of the active component. The sorbent HK-1S, which is the spent sorbent of HK-1 and obtained from the CO₂ capture pilot plant installed in a coal-fired power plant, also showed excellent physical properties and high saturation chlorine sorption capacity similar to that of a fresh one. In the fluidized-bed test, HK-1 and HK-1S reduced HCl concentration from hundreds ppmv to a few ppmv at 300–500 °C and 20 bar. Therefore, it can be concluded that both fresh and spent potassium-based CO₂ sorbents can be applied as an HCl sorbent for fluidized-bed reactor to remove HCl to a few ppmv level from the coal- or biomass-derived syngas at hot temperatures and HCl removal using spent CO₂ sorbent can be an advisable approach in economic and environmental point of view.

ACKNOWLEDGEMENTS

This work was supported by Energy Efficiency and Resources R&D program (2008CCD11P040000 and 2011201020004A) under the Ministry of Trade, Industry & Energy, Republic of Korea. The authors also would like to thank the Korea Electric Power Corpo-

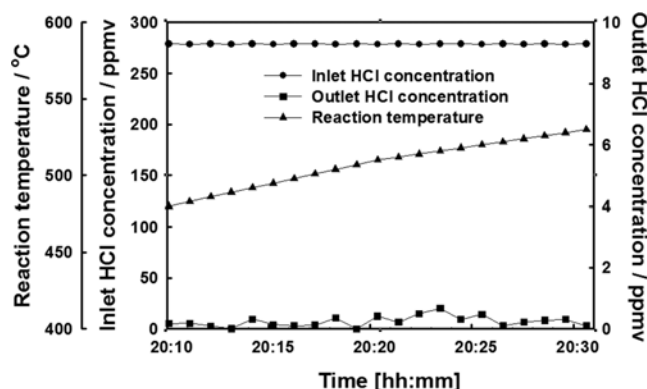


Fig. 6. The HCl removal performance of the spent potassium-based CO₂ sorbent in the bench-scale bubbling fluidized-bed reactor at 460–500 °C and 20 bar.

ration (KEPCO) and the Korea Western Power Company, Ltd. for supporting the program.

REFERENCES

1. "DOE/NETL advanced carbon dioxide capture R&D program: Technology update," National Energy Technology Laboratory, U.S. Department of Energy (2010).
2. Finkenrath, M. "Cost and Performance of Carbon Dioxide Capture from Power Generation," OECD/IEA (2011).
3. Gerdes, K. "Current and future technologies for gasification-based power generation," DOE/NETL-2009/1389, National Energy Technology Laboratory (2009).
4. "Preliminary Feasibility Analysis of RTI Warm Gas Cleanup (WGCU) Technology" Nexant (2007).
5. S. H. Kang, S. J. Lee, W. H. Jung, S. W. Chung, Y. Yun, S.-H. Jo, Y. C. Park and J.-I. Baek, *Korean J. Chem. Eng.*, **30**(1), 67 (2013).
6. Y. C. Park, S.-H. Jo, H.-J. Ryu, J.-H. Moon, C.-K. Yi, Y. Yoon and J.-I. Baek, *Korean J. Chem. Eng.*, **29**(12), 1812 (2012).
7. S. Y. Jung, J. J. Park, S. J. Lee, H. K. Jun, S. C. Lee and J. C. Kim, *Korean J. Chem. Eng.*, **27**(5), 1428 (2010).
8. S. Cheah, D. L. Carpenter and K. A. Magrini-Bair, *Energy Fuels*, **23**(11), 5291 (2009).
9. Y. Ohtsuka, N. Tsubouchi, T. Kikuchi and H. Hashimoto, *Powder Technol.*, **190**, 340 (2009).
10. C. S. Chyang, Y.-L. Han and Z.-C. Zhong, *Energy Fuels*, **23**, 3948 (2009).
11. B. Coda, M. Aho, R. Berger and K. R. G. Hein, *Energy Fuels*, **15**, 680 (2001).
12. C. E. Weinell, P. J. Jensen, K. Dam-Johansen and H. Livbjerg, *Ind. Eng. Chem. Res.*, **31**, 164 (1992).
13. J. Partanen, P. Backman, R. Backman and M. Hupa, *Fuel*, **84**(12-13), 1674 (2005).
14. W. Duo, N. F. Kirkby, J. P. K. Seville, J. H. A. Kiel, A. Bos and H. Den Uil, *Chem. Eng. Sci.*, **51**, 2541 (1996).
15. N. Verdone and P. De Filippis, *Chem. Eng. Sci.*, **61**, 7487 (2006).
16. B. Dou, J. Gao, S. W. Baek and X. Sha, *Energy Fuels*, **17**, 874 (2003).
17. B. Dou, J. Gao and X. Sha, *Fuel Process. Technol.*, **72**, 23 (2001).
18. G. N. Krishnan, R. P. Gupta, A. Canizales, S. Sheluka and R. Ayala, In: Schmidt, E., P. Gäng, T. Pilz and A. Dittler, Eds. "High Temperature Gas Cleaning" Karlsruhe: G. Braun Printconsult GmbH, 405 (1996).
19. M. Nunokawa, M. Kobayashi and H. Shirai, In: Dittler, A, G. Hemmer and G. Kasper, Eds. "High Temperature Gas Cleaning, Vol. II" Karlsruhe: G. Braun Printconsult GmbH, 684 (1999).
20. J. B. Lee, J.-I. Baek, C. K. Ryu, C. K. Yi, S. H. Jo and S. H. Kim, *Ind. Eng. Chem. Res.*, **47**, 4455 (2008).
21. J. B. Lee, C. K. Ryu, J.-I. Baek, J. H. Lee, T. H. Eom and S. H. Kim, *Ind. Eng. Chem. Res.*, **47**, 4465 (2008).
22. J.-I. Baek, C. K. Ryu, J. Ryu, J.-W. Kim, T. H. Eom, J. B. Lee and J. Yi, *Energy Fuels*, **24**, 5757 (2010).
23. J. B. Lee, T. H. Eom, B. S. Oh, J.-I. Baek, J. Ryu, W. S. Jeon, Y. H. Wi and C. K. Ryu, *Energy Procedia*, **4**, 1494 (2011).